THE JOURNAL OF PHYSICAL CHEMISTRY B

Article

pubs.acs.org/JPCB

Polymorphism of Racemic Poly(L-lactide)/Poly(D-lactide) Blend: Effect of Melt and Cold Crystallization

Rui-Ying Bao, Wei Yang,* Wen-Rou Jiang, Zheng-Ying Liu, Bang-Hu Xie, and Ming-Bo Yang

College of Polymer Science and Engineering, Sichuan University, State Key Laboratory of Polymer Materials Engineering, Chengdu, 610065, Sichuan, China

ABSTRACT: The crystallization and melting behaviors and crystalline structure of melt and cold crystallized poly(L-lactide)/poly(D-lactide) (PLLA/PDLA) blend were investigated by differential scanning calorimetry (DSC) and wide-angle X-ray diffraction (WAXD), respectively. The isothermal crystallization kinetics during the melt and cold crystallization process were analyzed using the Avrami equation. The overall crystallization rate constant (k) of cold crystallization is much higher than that of melt crystallization. Moreover, k as a function of crystallization temperature shows different trends in melt and cold crystallization, indicating different crystallization mechanisms in the melt and cold crystallization. The polymorphic crystallization of homocrystallites (the transition crystallization temperature from δ to α form) is not altered by either the equimolar blending of PLLA and PDLA or the type of crystallization procedures, while the crystallization window for exclusive stereocomplex crystallites is widened from 170 °C for melt crystallization to 170−200 °C for cold crystallization. The stereocomplex crystallites are hard to form in both melt and cold crystallization at crystallization temperatures of 90 and 100 °C, and the crystallinity of stereocomplex crystallites for cold crystallization is higher than that of melt crystallization at temperatures above 110 °C. Especially, a pure and significantly higher crystallinity of stereocomplex crystallites can be achieved at 170−200 °C by cold crystallization. The results provide a huge possibility to control stereocomplex crystallization to enlarge its applications.

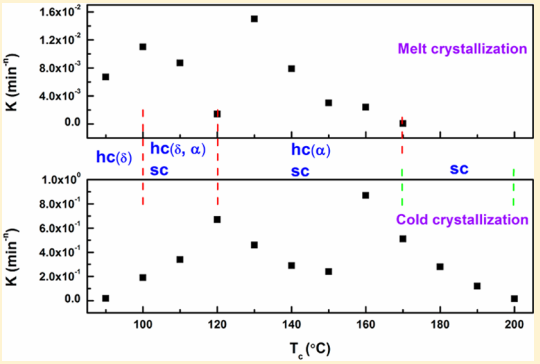

INTRODUCTION

Depending on the crystallization conditions, the common stereoisomer of poly(lactide) (PLA), i.e., poly(L-lactide) (PLLA) and poly(D-lactide) (PDLA), can crystallize in α, β, and γ polymorphs.[1,2] The most common crystal modification, the α form, generally produced from the cold, melt, or solution crystallization under normal conditions, is characterized by an orthorhombic (or pseudo-orthorhombic) unit cell packed by two antiparallel left-handed helical chains in a distorted 10_3 conformation.[3,4] The β form, adopting a 3_1 helical conformation, generally prepared upon stretching of the α form at high drawing ratio and high temperature.[5] The γ form has been obtained by Lotz and co-workers.[6] Recently, a disordered α (α' or δ) form has been found for the melt crystallized PLA at a crystallization temperature T_c lower than 100 °C, compared to the normal α crystallites produced at T_c higher than 120 °C.[7−13]

The PLLA/PDLA stereocomplex crystallites (sc) are another important crystal modification of PLA, generally produced in the crystallization of equimolar racemic PLLA/PDLA blend from the melt or solution.[14,15] One of the most characteristic features of sc is its high melting point, 50 °C higher than that of PLLA or PDLA homocrystallites (hc).[14,16] Because of its better physical properties, the PLA stereocomplex has drawn much attention since its first discovery by Ikada et al.[16] Stereocomplex crystallization has been proven to be one of the most effective methods to enhance the properties of PLA, including mechanical performance,[17−19] thermal stability,[20,21] and hydrolysis resistance.[22,23]

Many attempts have been made to identify the mechanism and effect of different parameters on the sc formation such as homopolymer molecular weight, blending ratio, optical purity, preparation methods, and crystallization conditions.[24−36] Generally, blending of PLLA and PDLA with high molecular weight is always accompanied by the hc crystallization along with the sc crystallization. For crystallization in bulk from the melt, the exclusive sc formation is limited to the PLLA and PDLA at least either of which has a molecular weight lower than 1×10^4 g mol^{-1}, whereas solely hc is achieved in the equimolar PLLA/PDLA blend where both polymers have molecular weights higher than 1×10^5 g mol^{-1}.[14,26]

In our previous work, it was first reported that pure sc can be achieved by a low temperature approach, i.e., processing at temperatures much lower than those adopted in conventional melt blending, using high-molecular-weight PLA that are difficult to form sc using conventional melt blending and solution casting methods. The process takes advantage of the temperature window at which only the sc can grow and the homopolymers can no longer crystallize, and develops a feasible way to overcome the molecular diffusion issue in the

Received: December 3, 2012
Revised: March 7, 2013
Published: March 11, 2013

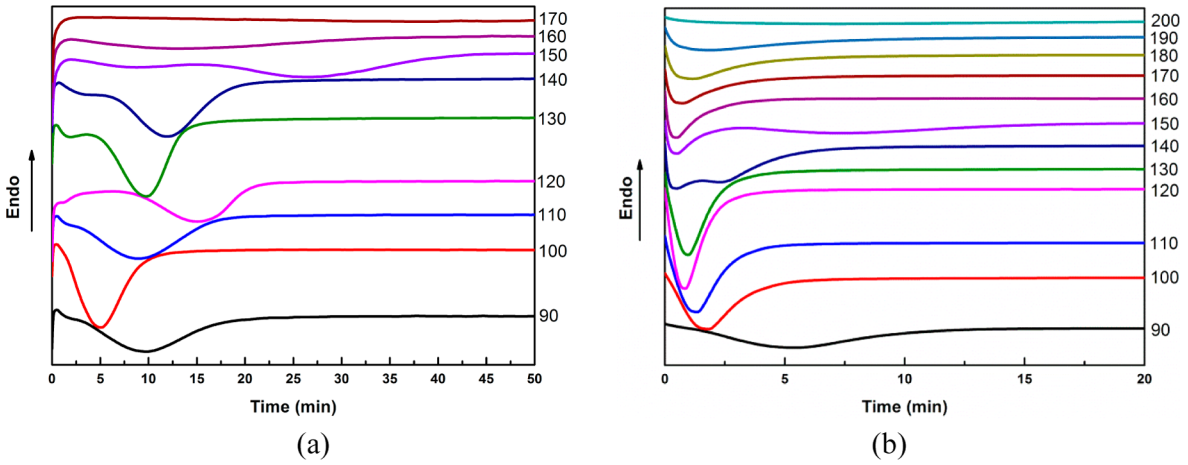

Figure 1. Crystallization exotherms for melt (a) and cold crystallized (b) PLLA/PDLA blend.

stereocomplex growth.[37] It implies that pure sc can be formed between the melting temperatures of hc and sc under certain conditions. In our opinion, the effect of processing temperature on the formation of sc in the low temperature approach is similar to that of cold crystallization if crystallization under quiescent conditions is considered.

The crystallization kinetics and crystalline polymorphism as well as the melting behavior are quite dependent on the crystallization conditions. The melt and cold crystallization behavior of PLLA have been carried out seriously,[8,38−45] and no research has been carried out on the effect of melt and cold crystallization on the crystallization kinetics and polymorphism of the PLLA/PDLA blend. In the present work, a comparison of the crystallization kinetics and crystalline structures as well as the melting behaviors of melt and cold crystallized PLLA/PDLA blend is made at a wide range of T_c. The effect of T_c on the crystallization kinetics as well as the efficiency to form a PLA stereocomplex is found to depend on whether the blend is brought to T_c by quenching from the melt (melt crystallization) or by heating from the glassy state (cold crystallization).

EXPERIMENTAL SECTION

PLLA (trade name 4032D, NatureWorks) was used in this study. The weight-averaged molecular weight (M_w) was 2.1 × 10^5 g mol^{-1}, and the polydispersity (PDI) was 1.7. The onset melting temperature and the peak melting temperatures of neat PLLA were 159.5 and 167.2 °C, measured by differential scanning calorimetry at a heating rate of 10 °C/min. For PDLA, M_w was 1.0 × 10^5 g mol^{-1} and the PDI was 1.7. The onset melting temperature and the peak melting temperature were 156.8 and 166.1 °C.

A racemic PLLA/PDLA blend at 1:1 weight ratio was prepared by solution blending. Briefly, the separately prepared 1.0 g dL^{-1} solutions of PLLA and PDLA using dichloromethane as the solvent were mixed vigorously. Then, PLLA/PDLA blend was obtained by solvent evaporation at room temperature and further vacuum-drying for 24 h to remove the residual solvent.

The overall crystallization behavior of PLLA/PDLA blend was monitored by differential scanning calorimetry (DSC) using a DSC Q20 (TA Instruments, USA) under a nitrogen gas flow of 50 mL min^{-1}. In the melt crystallization, the sample was first melted at 270 °C for 2 min to remove the thermal history. Then, it was cooled to the desired crystallization temperature (T_c = 90−170 °C) at 60 °C/min for an isothermal melt-crystallization period of 60 min. For the cold crystallization, the sample was first melted at 270 °C for 2 min to remove the thermal history. The sample was quenched from the melt into liquid nitrogen in order to obtain the amorphous sample. Then, the amorphous sample was heated to the desired crystallization temperature (T_c = 90−200 °C) at 200 °C/min for an isothermal cold-crystallization period of 60 min. After the completion of crystallization, the sample was reheated to 270 °C at 10 °C/min to examine the effect of a given isothermal history.

Relative crystallinity development is directly proportional to the evolution of heat released during the crystallization process. This relationship is depicted as

$$x_t = \frac{\int_0^t (dH/dt)\, dt}{\int_0^\infty (dH/dt)\, dt} \quad (1)$$

Isothermal crystallization kinetics of PLLA/PDLA blend can be described by the classical Avrami equation as follows:

$$1 - x_t = \exp(-kt^n) \quad (2)$$

where x_t is the relative crystallinity, n is the Avrami exponent that is normally an integer between 1 and 4, k is the overall crystallization rate constant, and t is the crystallization time. Applying logarithmic properties to both sides of eq 2, the following equation can be obtained:

$$\log[-\ln(1 - x_t)] = n \log t + \log k \quad (3)$$

The values of k and n can be calculated from the linear fitting of $\log[-\ln(1 - X_t)]$ versus $\log t$, and a linear portion of about 3−20% of relative crystallinity was used to obtain n and k.

After the completion of crystallization, the sample was quenched at 0 °C for 5 min, and the crystalline structure of PLLA/PDLA blend melt or cold crystallized at different T_c was investigated by wide-angle X-ray diffraction (WAXD). WAXD profiles were recorded on a DX-1000 X-ray diffractometer (Dandong Fanyuan Instrument Co. LTD) using a Cu Kα radiation source (λ = 0.154 056 nm, 40 kV, 25 mA) in the scanning angle range of 2θ = 5−50° at a scan speed of 3°/min. The crystallinities of the homocrystallites (X_c(hc)) and stereocomplex crystallites (X_c(sc)) were determined from WAXD profiles according to the procedure reported by Tsuji

dx.doi.org/10.1021/jp311878f | J. Phys. Chem. B 2013, 117, 3667−3674

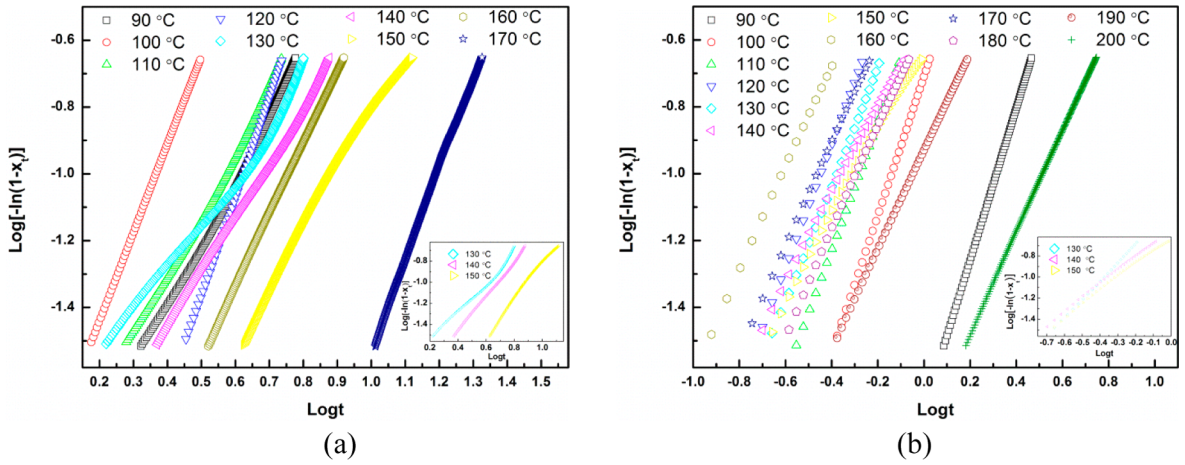

Figure 2. Avrami plots for melt (a) and cold crystallization (b) of PLLA/PDLA blend.

et al.[24,25] The fraction of sc, f_{sc}, can be obtained from the following equation

$$f_{sc} = \frac{X_c(sc)}{X_c(hc) + X_c(sc)} \quad (4)$$

RESULTS AND DISCUSSION

Crystallization Behavior for Melt and Cold Crystallized PLLA/PDLA Blend. Figure 1 shows the crystallization exotherms for melt and cold crystallized PLLA/PDLA blend. For melt crystallized PLLA/PDLA blend in Figure 1a, the rate of crystallization decreases with increasing T_c in the range 100−150 °C (except T_c of 120 °C) and 160−170 °C, respectively. At T_c higher than 170 °C, no exothermal peak can be observed and the DSC curves are not presented here. Moreover, at T_c of 130, 140, and 150 °C, the exothermal peak is asymmetric; i.e., a narrow peak appears in a short time, followed by a broad one depicted in all of the curves. For cold crystallized PLLA/PDLA blend in Figure 1b, the rate of crystallization increases with increasing T_c in a range of 90−120 °C, suggesting a growth-controlled regime, and the rate of crystallization decreases with increasing T_c in a range of 120−150 and 160−200 °C, respectively. At T_c higher than 200 °C, no exothermal peak can be observed. Moreover, at T_c of 140 and 150 °C, the exothermal peak is asymmetric. Compared with that of melt crystallization, the rate of cold crystallization is higher. Moreover, the cold crystallization of PLLA/PDLA blend can take place in a wider and higher temperature zone compared with the melt crystallization process. Only when the temperature is lower than 170 °C, the crystallization exothermic peak can be observed on the melt crystallization curves. However, this T_c limit rises to 200 °C for the cold crystallization.

Figure 2 shows Avrami plots for the melt and cold crystallization of PLLA/PDLA blend. The common method of the analysis of isothermal crystallization is to determine the overall crystallization rate constant k and the exponent n from the plot of $\log[-\ln(1 - X_t)]$ versus log time, which is expected to be linear. However, Avrami plots do not display a straight line at T_c of 130, 140, and 150 °C for the melt crystallization of PLLA/PDLA blend, as shown by the inset of Figure 2a, consistent with the asymmetric exothermal peak as shown in Figure 1a. The similar nonstraight line can be observed at T_c of 140 and 150 °C for the cold crystallization of PLLA/PDLA blend, as shown by the inset of Figure 2b, also coincident with an asymmetric exothermal peak as shown in Figure 1b.

Crystallization kinetics parameters for the melt and cold crystallization of PLLA/PDLA blend were obtained from the Avrami plots, and are summarized in Table 1. Crystallization

Table 1. Crystallization Kinetics Parameters for Melt and Cold Crystallized PLLA/PDLA Blend

	melt crystallization		cold crystallization	
T_c (°C)	n	$t_{1/2}$ (min)	n	$t_{1/2}$ (min)
90	1.9	9.4	2.3	4.8
100	2.6	4.9	2.1	1.8
110	1.9	8.6	1.9	1.4
120	3	13.6	1.8	1
130	1.4	8.7	1.7	1.2
140	1.6	10.9	1.3	2.2
150	1.7	23	1.3	6
160	2.1	14.4	1.5	0.97
170	2.7	31.9	1.5	1.4
180			1.5	2
190			1.5	3.6
200			1.5	12.2

half-time ($t_{1/2}$), defined as the time spent from the onset of the crystallization to the point where the crystallization is 50% completed, has been normally used in the analysis of crystallization kinetics and is taken as a measure of the overall rate of crystallization. For melt crystallized PLLA/PDLA blend, $t_{1/2}$ roughly increases with increasing T_c in the range 100−150 °C but changes discontinuously with T_c and varies abruptly at T_c of 120 °C. $t_{1/2}$ of the cold crystallization decreases with increasing T_c in the 90−120 °C range and increases with increasing T_c at two higher different ranges of 130−150 and 160−200 °C, respectively. Moreover, $t_{1/2}$ for the cold crystallization is much lower than the corresponding values for melt crystallization, indicating a much faster overall crystallization rate for cold crystallization.

The overall crystallization rate constants (k) as a function of crystallization temperature (T_c) for melt and cold crystallized PLLA/PDLA blend are shown in Figure 3. The overall crystallization rate reflected by k is coincident with that of $t_{1/2}$. First, the value of k for cold crystallization is at least 1 order of magnitude larger than that of melt crystallized PLLA/PDLA

dx.doi.org/10.1021/jp311878f | J. Phys. Chem. B 2013, 117, 3667−3674

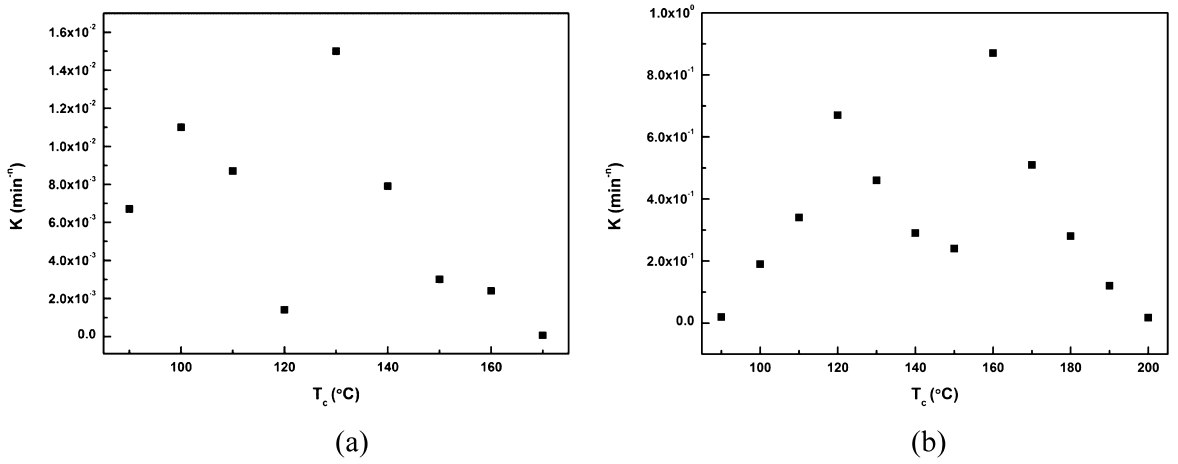

Figure 3. Overall crystallization rate constants (k) as a function of crystallization temperature (T_c) for melt (a) and cold crystallization (b) of PLLA/PDLA blend.

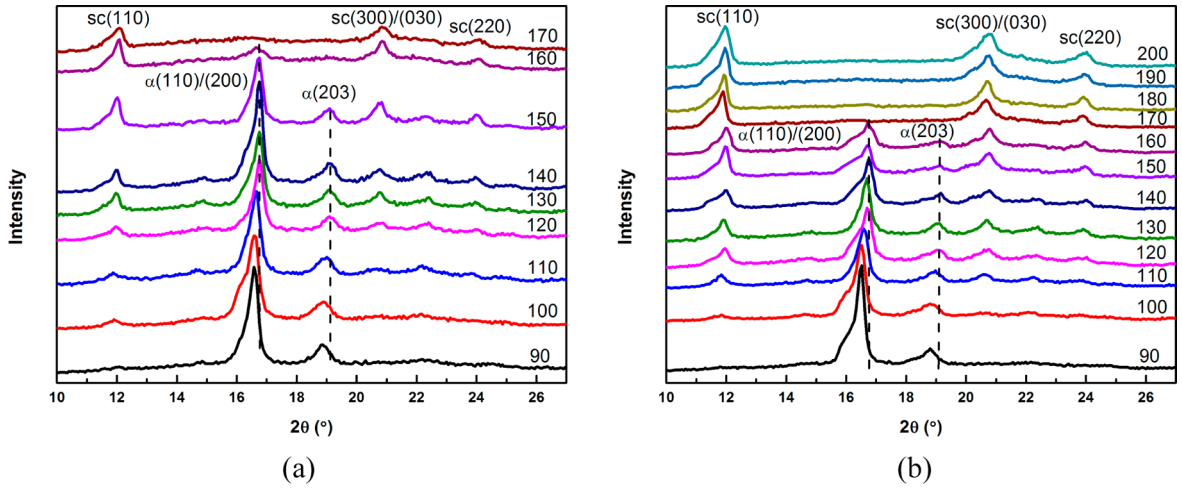

Figure 4. WAXD profiles of PLLA/PDLA blend melt (a) and cold crystallized (b) at different T_c.

blend. Second, k as a function of T_c shows different bell-shaped curves of crystal growth for melt and cold crystallized PLLA/PDLA blend. For melt crystallized PLLA/PDLA blend in Figure 3a, at T_c in the range 90−150 °C, the crystallization kinetics are discontinuous at T_c = 110−120 °C. Very different from the usual bell-shaped curve of polymer crystal growth, the curve of k as a function of T_c displays the first maximum at around 130 °C and the second at around 100 °C. Crystallization kinetics for the melt and cold crystallization of PLLA have been studied by a number of researchers. The maximum of the growth rate is observed at around 100 °C, and a second maximum is also observed at around 125 °C. The growth rate displays clear discontinuity at around 110−120 °C.[46] It has been reported that, when neat PLLA samples crystallize at temperatures lower than 100 °C, the δ form crystallites of PLLA form; when PLLA samples crystallize in the temperature region 100−120 °C, mixtures of α and δ crystallites form; at T_c higher than 120 °C, α crystallites form.[10] Obviously, the k as a function of T_c for the melt crystallization of PLLA/PDLA blend is similar to that of PLLA in the usual melt or cold crystallization, and the discontinuous kinetics is due to the different crystallization mechanism of homopolymers at high and low T_c. In other words, at T_c in the range 90−150 °C, k as a function of T_c for melt crystallization of PLLA/PDLA blend shows crystallization characteristics of hc exactly. At T_c of 160 and 170 °C, the k continues to reduce.

Different from the melt crystallization, as shown in Figure 3b, the k as a function of T_c for cold crystallized PLLA/PDLA blend shows two different bell-shaped crystal growth curves located at roughly 90−150 and 150−200 °C, respectively. At T_c in the range 90−150 °C, k typically shows a maximum at 120 °C defined as the optimum T_c. Accordingly, diffusion is the controlling factor at lower temperatures, whereas the rate of nucleation dominates at higher temperatures. At T_c in the range 160−200 °C, k decreases with increasing T_c.

Crystalline Structure and Melting Behavior for Melt and Cold Crystallized PLLA/PDLA Blend. WAXD profiles of PLLA/PDLA blend melt and cold crystallized at different T_c are shown in Figure 4. For melt crystallized PLLA/PDLA blend in Figure 4a, at T_c of 90 °C, the diffraction peaks at 2θ values of 16 and 18.4, which correspond to the (200) and/or (110) planes, and (203) planes of the α or δ form of PLLA or PDLA homocrystallites,[47] can be observed, whereas no sc diffraction peaks at 2θ values of 11.6, 20.6, and 23.5°, assigned to the (110) planes, (300) and/or (030) planes, and (220) planes,[15] are observed. At T_c of 100−160 °C, both the diffraction peaks of hc and sc can be observed. Moreover, sc(110), the strongest diffraction peak of sc, is stronger than α(110)/(200) of hc at

dx.doi.org/10.1021/jp311878f | J. Phys. Chem. B 2013, 117, 3667−3674

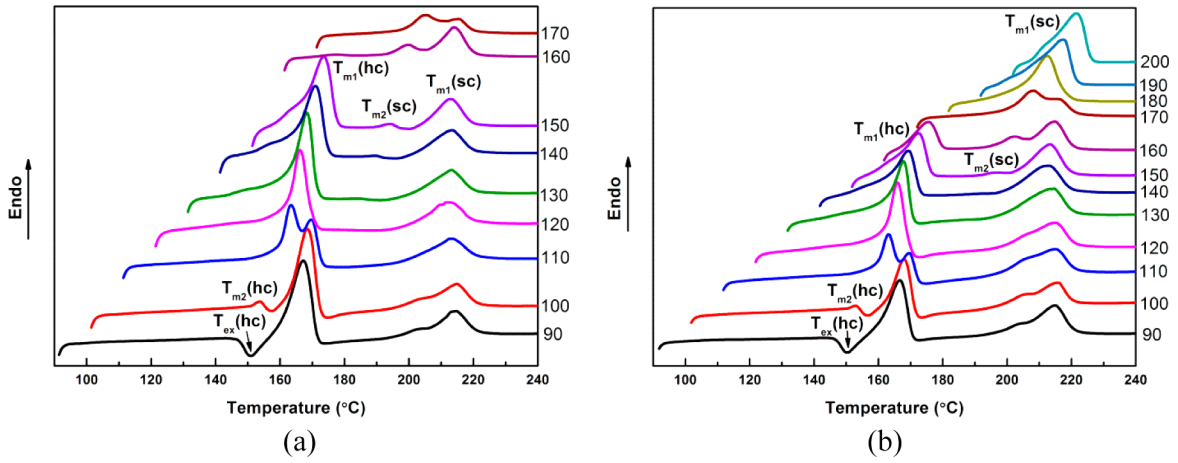

Figure 5. Melting curves of PLLA/PDLA blend melt (a) and cold crystallized (b) at different T_c.

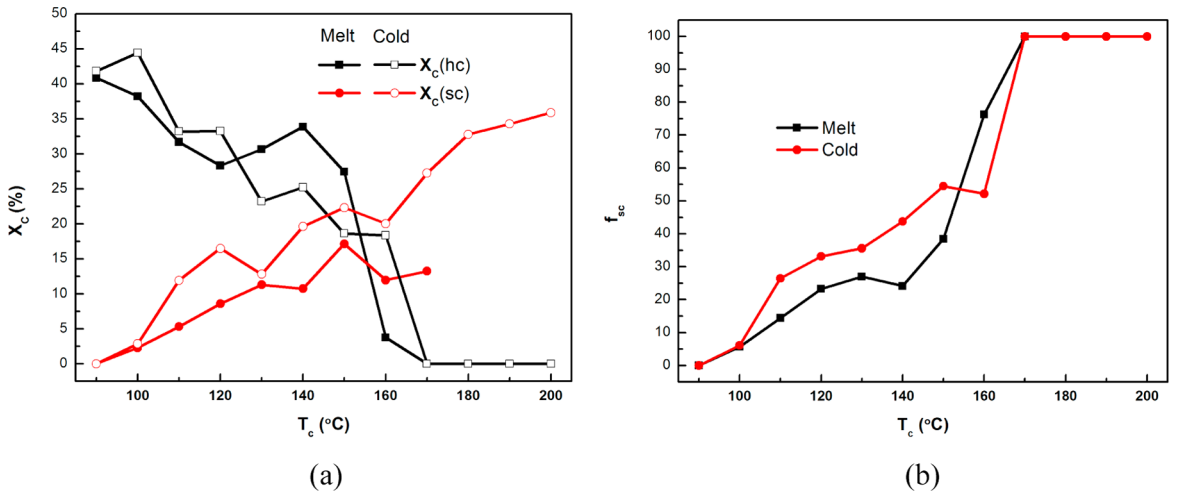

Figure 6. The effect of T_c on the crystallinity (a) and the fraction of the sc (b) by the WAXD method for melt and cold crystallized PLLA/PDLA blend.

160 °C, which is different from the situation below 160 °C. When T_c is lower than 120 °C, the (200)/(110) and (203) peaks indicated by dashed lines (Figure 4a) shifted to lower 2θ; When T_c is above 120 °C, the (200)/(110) and (203) peaks remained the same. This means that there is a disorder-to-order (δ to α) form transition temperature near 120 °C. Above the transition temperature, only the α form formed. Below 120 °C, the (200)/(110) and (203) reflections changed because of the coexistences of the δ and α forms. Melting curves of PLLA/PDLA blend melt and cold crystallized at different T_c are shown in Figure 5. Clearly, the melting behaviors of melt and cold crystallized PLLA/PDLA blend are strongly dependent on T_c. For melt crystallized PLLA/PDLA blend in Figure 5a, at T_c in the range 90−160 °C, two main endothermic peaks are clearly observed at around 170 and 210 °C, indicating the melting of hc and sc, respectively. It should be noted that, at T_c of 90 and 100 °C, the strong sc melting peaks with a weak shoulder are shown on melting curves, though no or very weak sc diffraction peaks can be observed in Figure 4a. These strong sc melting peaks may be due to the sc formed during DSC heating after melting of hc,[34,35,48] and then the weak shoulder emerges. Additionally, at T_c of 90 °C, a small exothermic peak (donated as T_{ex}(hc)) appears prior to the dominant melting peak of hc (T_{m1}(hc)) because of the phase transition from disordered δ form crystallites to the ordered α form one during heating scan.[11] However, at T_c of 100 and 110 °C, the small exotherm disappears, and two endotherms of hc (T_{m2}(hc) and T_{m1}(hc)) are present, indicating the formation of δ and α forms. Until T_c reaches 120−160 °C, only one endotherm of hc (T_{m1}(hc)) appears, suggesting only the crystallization of the α form occurs. The above polymorphic structures indicated by DSC results are consistent with those of WAXD analysis, which demonstrate that the transition T_c from δ to α form is not altered by the equimolar blending of PLLA and PDLA.

As shown in Figure 4a, with increasing T_c to 170 °C, only the diffraction peaks of sc can be observed, suggesting that complete sc while no hc is achieved. At T_c of 170 °C, the melting curves in Figure 5a show only one peak at around 210 °C, also suggesting that complete sc with no hc is achieved. Moreover, at T_c of 150, 160, and 170 °C, a double melting peak behavior of sc (T_{m2}(sc) and T_{m1}(sc)) is observed above 200 °C, which is much higher than the melting temperature of hc. Thus, both peaks have a stereocomplex nature. The double stereocomplex melting peak behavior after isothermal crystallization in DSC has been previously reported by Saeidlou et al.,[49] and it can be associated with a dual crystalline morphology for PLA stereocomplex comprising a spherulitic and a network structure revealed by optical microscopy observations. The

dx.doi.org/10.1021/jp311878f | J. Phys. Chem. B 2013, 117, 3667−3674

lower temperature melting peak is associated to the network structure, and the higher temperature peak is the characteristic peak for spherulite melting.

For cold crystallized PLLA/PDLA blend, at T_c in the range 90−160 °C, the diffraction characteristics in Figure 4b are not altered by cold crystallization compared to that of melt crystallized PLLA/PDLA blend at the corresponding T_c, with an exception that the sc(110) peak is still weaker than α(110)/(200) of hc at 160 °C. The multiple melting behavior characteristics in Figure 5b are similar to that of melt crystallized PLLA/PDLA blend at corresponding T_c. The similarities of the diffraction and multiple melting behavior characteristics between melt and cold crystallization indicate that the polymorphic crystallization (the transition T_c from δ to α form) is not altered by the type of crystallization procedures as well. At T_c of 160 °C, the melting peak of hc is obvious, and which is very weak for melt crystallized PLLA/PDLA blend. With T_c increasing to 170−200 °C, only the diffraction peaks of sc appear in Figure 4b, and only one endotherm of sc (T_{m1}(sc)) can be observed on melting curves in Figure 5b. Considering the effect of the type of crystallization procedures on the sc formation, it can be seen that the T_c for complete sc formation with no hc in melt crystallization is 170 °C, and that in cold crystallization is in the range 170−200 °C. It means that the complete sc formation can take place at a wider and higher T_c range for cold crystallized PLLA/PDLA blend compared with the melt crystallization process. The results indicate that, although no difference can be observed in the nature and temperature range of the diffraction characteristics and multiple melting behaviors of hc between melt and cold crystallized PLLA/PDLA blend, the crystallization window for exclusive sc is widened, especially in the higher temperature range.

Figure 6 shows the effect of T_c on the crystallinity and the fraction of the sc by the WAXD method for melt and cold crystallized PLLA/PDLA blend. At T_c of 90 °C, the crystallinity of the sc, X_c(sc), is 0%. At T_c of 110 °C, the values of X_c(sc) for melt and cold crystallized PLLA/PDLA blend are almost equal and below 3%, as shown in Figure 6a, and the fractions of sc represented by f_{sc} are similar in Figure 6b. Moreover, at T_c above 110 °C, significantly higher X_c(sc) values for cold crystallized PLLA/PDLA blend than that of melt crystallization can be observed in Figure 6a, and the values of f_{sc} are higher for cold crystallization except at T_c of 160 °C, as shown in Figure 6b. 100% sc can be observed at T_c of 170 °C for melt crystallization, and this T_c range expands to 170−200 °C for cold crystallization. Especially, in the case of cold crystallization, X_c(sc) increases drastically to above 30% at T_c higher than 170 °C.

DISCUSSION

The crystallization kinetics and the crystalline structure of PLLA/PDLA blend are quite dependent on the crystallization conditions including T_c and type of crystallization procedures. For melt and cold crystallized PLLA/PDLA blend in this work, differences in crystallization kinetics are observed due to the difference in initial state. The similarities of the crystalline structure by WAXD results and multiple melting behaviors over the entire isothermal temperature range for both melt and cold crystallization suggest that these observed differences may not be due to any significant differences in crystal form in the two methods.

For the melt crystallization of PLLA/PDLA blend, the sc can act as nucleation sites of hc and enhance the crystallization of hc significantly (heterogeneous nucleation).[50] sc would act as homogeneous nucleation sites for sc itself as well as heterogeneous nucleation sites for hc crystallization, or hc are formed epitaxially on the sc. There is a competition balance that existed between the hc crystallization of PLLA or PDLA chains and sc crystallization of PLLA/PDLA chains due to the sharing of the sc nucleation sites.[32] On the other hand, the increased hc crystallization disturbs the sc crystallization because of the crystallization competition between the homopolymer chains and stereocomplex chains. The mechanism may be proposed as follows. On the one hand, in melt crystallized PLLA/PDLA blend, the sc structure develops as the sc crystallinity increases. This structure is slightly disturbed by the crystal growth of hc. On the other hand, sc have been found to enhance the nucleation of crystallization but slightly interrupts the crystallization growth of hc.[51] For melt crystallized PLLA/PDLA blend in Figure 3a, at T_c in the range 90−150 °C, the k as a function of T_c for melt crystallized PLLA/PDLA blend shows crystallization characteristics of hc exactly, confirming the fact that the presence of sc as a nucleating agent does not affect the growth mechanism of hc.

For cold crystallized PLLA/PDLA blend in Figure 3b, k typically shows a maximum at 120 °C defined as the optimum T_c in the range 90−150 °C. Accordingly, diffusion is the controlling factor at lower temperatures, whereas the rate of nucleation dominates at higher temperatures. At T_c lower than 120 °C, the value of k increases with increasing T_c, while the $t_{1/2}$ value increases with T_c. These results indicate that, with the increase of T_c, the crystallization rate increases. This can be explained by the fact that the cold crystallization shows a temperature dependence, which is a characteristic of growth controlled crystallization. Nevertheless, even if no crystal growth process takes place on cooling in the case of cold crystallization, a certain number of nuclei is expected to be formed during this process whose number could depend on the cooling rate.[52] The formed nuclei are supposed to consist of hc and sc nuclei. The nuclei exist already in the cold crystallization case, and the regularization and growth of the hc and sc occur more easily, and the crystallization of the α and δ form of hc depends on T_c. The faster kinetics for the cold crystallized PLLA/PDLA blend is further confirmed in Figure 3, which shows the value of k for cold crystallization is at least 1 order of magnitude larger than that of melt crystallization. Tsuji et al.[45] also reported a shorter time for PLLA cold crystallization than in melt crystallization due to the higher nucleation density in the former. The synchronous existence of hc and sc nuclei makes the sc crystallization hardly be disturbed, which shows significantly higher X_c(sc) values for the cold crystallized PLLA/PDLA blend than that of melt crystallization above T_c of 110 °C in Figure 6a. Maybe the faster kinetics of sc make the value of k show the kinetics of sc, and the dependence of the α and δ forms of hc on T_c is covered. In addition, at T_c of 90 and 100 °C, the X_c(sc) is very low and similar for melt and cold crystallization. The possible reason is that the decreased chain mobility at low T_c makes the PDLA chains hard to confront with PLLA chains, and then the growth of sc is disturbed seriously due to the lack of helical pairs of PLLA and PDLA chains. Tsuji et al.[27] investigated the crystallization behavior of PLLA/PDLA blends and found that solely hc mixtures of PLLA and PDLA are synchronously and separately formed during isothermal crystallization in the T_c range 90−130 °C, irrespective of blending ratio, whereas, in addition to hc, sc

dx.doi.org/10.1021/jp311878f | J. Phys. Chem. B 2013, 117, 3667−3674

are formed in the equimolar blends at T_c above 150 and 160 °C.

As shown in Figure 2, Avrami plots do not display a straight line at T_c of 130, 140, and 150 °C for melt crystallized PLLA/PDLA blend, and similar nonstraight lines can be observed at T_c of 140 and 150 °C for cold crystallization. Usually, the secondary crystallization processes at the end of crystallization produce nonlinearity in the Avrami plot at the end of crystallization.[53] The secondary crystallization can usually be identified by the deviation of an Avrami plot at the nonlinear stage where the spherulites may impinge with each other and their growth may either be related to subsidiary lamellae or to the thickening of lamellae. However, the occurrence of secondary crystallization is impossible at the beginning of crystallization in the 3−20% relative conversion range. Combining with the asymmetric exothermal peak observed in Figure 1, the reason for it is the time dependence of at least one of the two kinetic parameters in the Avrami equation, either the crystallization rate (which contains the nucleation and growth rates) or the exponent n. The crystallization rate of sc is much faster than that of hc;[28] i.e., the narrow peak appearing at short time reflects the crystallization of sc mainly, and the followed broad one results from the crystallization of hc epitaxial on the sc, or the simultaneous crystallization of hc and sc. Then, Avrami plots do not display a straight line. Moreover, the synchronous existence of hc and sc nuclei may make the crystallization of hc at T_c of 130 °C occur at the beginning of cold crystallization, and Avrami plots displays a straight line, different from that for melt crystallization.

The comparison of the crystallization kinetics between melt and cold crystallization means that, even the hc crystallization disturbs the sc crystallization because of the crystallization competition between the homopolymer chains and stereocomplex chains for cold crystallization, it is more weak compared to that in melt crystallization, in which the sharing of sc nuclei and chains exists. The sc nuclei formed during melt crystallization act as the nucleating agent for the hc and sc crystallization, resulting in rapid completion of crystallization in the blend. However, the polymorphic crystallization of hc (the transition T_c from δ to α form) is not altered by either the equimolar blending of PLLA and PDLA or the type of crystallization procedures. Tsuji et al.[27] also reported that the transition T_c from δ to α form is not altered by the synchronous and separate crystallization of PLLA and PDLA.

The crystallization window is also widened for cold crystallization compared to that of melt crystallization, especially in the higher temperature range. The melting temperature of sc is 50 °C higher than that of hc. This temperature window between the melting temperature of the sc and the melting temperature of hc, much wider than any other polymorphic polymer known, can be used to produce the sc when the homopolymers can no longer crystallize. The high processing temperature window in which sc can be produced and the homopolymers can no longer crystallize is really important for the sc formation. In this work, the onset melting temperature and the melting temperatures are 159.5 and 167.2 °C for neat PLLA and 156.8 and 166.1 °C for neat PDLA, respectively, measured by DSC at a heating rate of 10 °C/min. At T_c of 160 °C for melt crystallization, T_c is close to the melting temperature of hc, and hc are hard to form. With T_c increased to 170 °C, T_c is higher than the melting temperature of hc, and only the crystallization of sc is possible. Nucleation and growth dominate the crystallization process.[54,55] With further increasing of T_c, sc cannot be formed, probably because the increasing of the chain mobility is overcome by the great decrease of the formed nucleation density, and the sc crystallization rate decreases at a low degree of supercooling. Then, only when temperature is lower than 170 °C, the crystallization exothermic peak can be observed on the melt crystallization curves. Yang et al.[56] also found sc can be observed to develop during melt crystallization only at 170 °C but not at 200 °C, due to the presence of low and high populations of helical pairs, and adequate population of racemic helical pairs is needed for formation of their mesomorphic clusters in the melt matrix as precursors of sc nuclei.

The synchronous existence of hc and sc nuclei makes the crystallization of hc occur more easily at 160 °C for cold crystallization than melt crystallization; then, f_{sc}(hc) is relatively lower than that of melt crystallization, as shown in Figure 6b. At the same time, the existence of the sc nuclei makes the T_c limit of complete sc rise to 200 °C for the cold crystallization. When T_c is between 180 and 200 °C, exclusive sc can be formed by cold crystallization, although no discernible crystallization is observed during melt crystallization under the corresponding T_c. The T_c higher than 200 °C approaches the melting temperature of sc, and sc are hard to form and live even during cold crystallization. Moreover, in the temperature window in which only sc can crystallize, complete sc form, as shown in Figure 6b, and X_c(sc) increases significantly as shown in Figure 6a due to the disappearance of crystallization competition from hc. The results indicate that the effect of the type of crystallization procedures on the efficiency of stereocomplex formation is quite different. These data reveal that the sc crystallinity of PLLA/PDLA blend can be controlled by changing the type of crystallization procedures, and cold crystallization can provide a versatile method for achieving a high fraction of sc in the PLLA/PDLA blend. These results demonstrate the profound effect of thermal history on the crystallization characteristics in the PLLA/PDLA blend and are extremely significant for understanding the effect of processing conditions on the formation of sc, physical, and mechanical properties of this bio based polymer.

CONCLUSION

A comparison of crystallization behavior for melt and cold crystallized PLLA/PDLA blend is investigated. Significant differences in crystallization kinetics during melt and cold crystallization indicate different crystallization mechanisms in melt and cold crystallization. The polymorphic crystallization of hc (the transition T_c from δ to α form) is not altered by either the equimolar blending of PLLA and PDLA or the type of crystallization procedures, while the crystallization window for sc is widened in cold crytallization, especially at the higher temperature range. When the T_c is between 180 and 200 °C, a pure PLA stereocomplex can be formed in the blend by cold crystallization, although no discernible crystallization is observed during melt crystallization under the same condition. The effects of melt crystallization and cold crystallization on the crystalline structure of PLLA/PDLA blend also show that the cold crystallization is more beneficial to the formation of PLA stereocomplex at T_c above 110 °C.

AUTHOR INFORMATION

Corresponding Author

*Phone: + 86 28 8546 0130. Fax: + 86 28 8546 0130. E-mail: weiyang@scu.edu.cn.

Notes

The authors declare no competing financial interest.

■ ACKNOWLEDGMENTS

This work was supported by the National Natural Science Foundation of China (NNSFC Grants 51033003, 51121001), the MOST (Grant No. 2011CB606006), and the Fundamental Research Funds for the Central Universities (Grant No. 2011SCU04A03).

■ REFERENCES

(1) Pan, P.; Inoue, Y. *Prog. Polym. Sci.* **2009**, *34* (7), 605−640.
(2) Pan, P.; Yang, J.; Shan, G.; Bao, Y.; Weng, Z.; Cao, A.; Yazawa, K.; Inoue, Y. *Macromolecules* **2012**, *45* (1), 189−197.
(3) Aleman, C.; Lotz, B.; Puiggali, J. *Macromolecules* **2001**, *34* (14), 4795−4801.
(4) Sasaki, S.; Asakura, T. *Macromolecules* **2003**, *36* (22), 8385−8390.
(5) Sawai, D.; Takahashi, K.; Sasashige, A.; Kanamoto, T.; Hyon, S.-H. *Macromolecules* **2003**, *36* (10), 3601−3605.
(6) Cartier, L.; Okihara, T.; Ikada, Y.; Tsuji, H.; Puiggali, J.; Lotz, B. *Polymer* **2000**, *41* (25), 8909−8919.
(7) Kawai, T.; Rahman, N.; Matsuba, G.; Nishida, K.; Kanaya, T.; Nakano, M.; Okamoto, H.; Kawada, J.; Usuki, A.; Honma, N.; et al. *Macromolecules* **2007**, *40* (26), 9463−9469.
(8) Zhang, J.; Duan, Y.; Sato, H.; Tsuji, H.; Noda, I.; Yan, S.; Ozaki, Y. *Macromolecules* **2005**, *38* (19), 8012−8021.
(9) Zhang, J.; Tashiro, K.; Domb, A. J.; Tsuji, H. *Macromol. Symp.* **2006**, *242* (1), 274−278.
(10) Zhang, J.; Tashiro, K.; Tsuji, H.; Domb, A. J. *Macromolecules* **2008**, *41* (4), 1352−1357.
(11) Pan, P.; Kai, W.; Zhu, B.; Dong, T.; Inoue, Y. *Macromolecules* **2007**, *40* (19), 6898−6905.
(12) Pan, P. J.; Zhu, B.; Kai, W. H.; Dong, T.; Inoue, Y. *Macromolecules* **2008**, *41* (12), 4296−4304.
(13) Pan, P.; Liang, Z.; Zhu, B.; Dong, T.; Inoue, Y. *Macromolecules* **2009**, *42* (9), 3374−3380.
(14) Tsuji, H. *Macromol. Biosci.* **2005**, *5* (7), 569−597.
(15) Cartier, L.; Okihara, T.; Lotz, B. *Macromolecules* **1997**, *30* (20), 6313−6322.
(16) Ikada, Y.; Jamshidi, K.; Tsuji, H.; Hyon, S. H. *Macromolecules* **1987**, *20* (4), 904−906.
(17) Rathi, S.; Chen, X.; Coughlin, E. B.; Hsu, S. L.; Golub, C. S.; Tzivanis, M. J. *Polymer* **2011**, *52* (19), 4184−4188.
(18) Rathi, S. R.; Coughlin, E. B.; Hsu, S. L.; Golub, C. S.; Ling, G. H.; Tzivanis, M. J. *Polymer* **2012**, *53* (14), 3008−3016.
(19) Tsuji, H.; Ikada, Y. *Polymer* **1999**, *40* (24), 6699−6708.
(20) Tsuji, H.; Fukui, I. *Polymer* **2003**, *44* (10), 2891−2896.
(21) Purnama, P.; Lim, S.; Jung, Y.; Kim, S. *Macromol. Res.* **2012**, *20* (6), 545−548.
(22) Tsuji, H. *Polymer* **2000**, *41* (10), 3621−3630.
(23) Tsuji, H. *Biomaterials* **2003**, *24* (4), 537−547.
(24) Tsuji, H.; Yamamoto, S. *Macromol. Mater. Eng.* **2011**, *296* (7), 583−589.
(25) Tsuji, H.; Nakano, M.; Hashimoto, M.; Takashima, K.; Katsura, S.; Mizuno, A. *Biomacromolecules* **2006**, *7* (12), 3316−3320.
(26) Tsuji, H.; Ikada, Y. *Macromolecules* **1993**, *26* (25), 6918−6926.
(27) Tsuji, H.; Tashiro, K.; Bouapao, L.; Hanesaka, M. *Polymer* **2012**, *53* (3), 747−754.
(28) Tsuji, H.; Tezuka, Y. *Biomacromolecules* **2004**, *5* (4), 1181−1186.
(29) Purnama, P.; Kim, S. H. *Macromolecules* **2010**, *43* (2), 1137−1142.
(30) Purnama, P.; Hyun Kim, S. *Polym. Int.* **2012**, *61* (6), 939−942.
(31) Purnama, P.; Jung, Y.; Kim, S. H. *Macromolecules* **2012**, *45* (9), 4012−4014.
(32) Sun, J.; Yu, H.; Zhuang, X.; Chen, X.; Jing, X. *J. Phys. Chem. B* **2011**, *115* (12), 2864−2869.
(33) Shao, J.; Sun, J.; Bian, X.; Cui, Y.; Li, G.; Chen, X. *J. Phys. Chem. B* **2012**, *116* (33), 9983−9991.
(34) Fujita, M.; Sawayanagi, T.; Abe, H.; Tanaka, T.; Iwata, T.; Ito, K.; Fujisawa, T.; Maeda, M. *Macromolecules* **2008**, *41* (8), 2852−2858.
(35) Zhang, J. M.; Tashiro, K.; Tsuji, H.; Domb, A. J. *Macromolecules* **2007**, *40* (4), 1049−1054.
(36) Brochu, S.; Prud'homme, R. E.; Barakat, I.; Jerome, R. *Macromolecules* **1995**, *28* (15), 5230−5239.
(37) Bao, R.-Y.; Yang, W.; Jiang, W.-R.; Liu, Z.-Y.; Xie, B.-H.; Yang, M.-B.; Fu, Q. *Polymer* **2012**, *53* (24), 5449−5454.
(38) Badrinarayanan, P.; Dowdy, K. B.; Kessler, M. R. *Polymer* **2010**, *51* (20), 4611−4618.
(39) Wang, Y.; Funari, S. S.; Mano, J. F. *Macromol. Chem. Phys.* **2006**, *207* (14), 1262−1271.
(40) Wasanasuk, K.; Tashiro, K. *Macromolecules* **2011**, *44* (24), 9650−9660.
(41) Zhang, J.; Tsuji, H.; Noda, I.; Ozaki, Y. *Macromolecules* **2004**, *37* (17), 6433−6439.
(42) Na, B.; Tian, N.; Lv, R.; Li, Z.; Xu, W.; Fu, Q. *Polymer* **2010**, *51* (2), 563−567.
(43) Na, B.; Zou, S.; Lv, R.; Luo, M.; Pan, H.; Yin, Q. *J. Phys. Chem. B* **2011**, *115* (37), 10844−10848.
(44) Vasanthan, N.; Ly, H.; Ghosh, S. *J. Phys. Chem. B* **2011**, *115* (31), 9556−9563.
(45) Tsuji, H.; Ikada, Y. *Polymer* **1995**, *36* (14), 2709−2716.
(46) Di Lorenzo, M. L. *Eur. Polym. J.* **2005**, *41* (3), 569−575.
(47) Hoogsteen, W.; Postema, A. R.; Pennings, A. J.; Ten Brinke, G.; Zugenmaier, P. *Macromolecules* **1990**, *23* (2), 634−642.
(48) Tsuji, H.; Del Carpio, C. A. *Biomacromolecules* **2003**, *4* (1), 7−11.
(49) Saeidlou, S.; Huneault, M. A.; Li, H.; Sammut, P.; Park, C. B. *Polymer* **2012**, *53* (25), 5816−5824.
(50) Yamane, H.; Sasai, K. *Polymer* **2003**, *44* (8), 2569−2575.
(51) Rahman, N.; Kawai, T.; Matsuba, G.; Nishida, K.; Kanaya, T.; Watanabe, H.; Okamoto, H.; Kato, M.; Usuki, A.; Matsuda, M.; et al. *Macromolecules* **2009**, *42* (13), 4739−4745.
(52) Salmerón Sánchez, M.; Mathot, V. B. F.; Vanden Poel, G.; Gómez Ribelles, J. L. *Macromolecules* **2007**, *40* (22), 7989−7997.
(53) Lorenzo, A. T.; Arnal, M. L.; Albuerne, J.; Müller, A. J. *Polym. Test.* **2007**, *26* (2), 222−231.
(54) Hoffman, J. D.; Miller, R. L. *Polymer* **1997**, *38* (13), 3151−3212.
(55) Sadler, D. M.; Gilmer, G. H. *Phys. Rev. Lett.* **1986**, *56* (25), 2708−2711.
(56) Yang, C.-F.; Huang, Y.-F.; Ruan, J.; Su, A.-C. *Macromolecules* **2012**, *45* (2), 872−878.